2026 Volume: 02 Issue: 02 www.ijrpa.com ISSN 2456-9995 Review Article

International Journal Research Publication Analysis

Page: 01-10

DEVELOPMENT OF A TRAJECTORY TRACKING ALGORITHM FOR UAVS

[*1]Thi Hong Nguyen, [1]Thi Thuy Tran, [2]Anh Duong Vu, [2]Hong Tien Nguyen, [2]Van Cong Tran, [2]Hong Son Tran, [2]Xuan Tuyen Do

[1]Master, Academy of Military Science and Technology, Hanoi, Vietnam.

[2]Master, Faculty of Aviation Engineering, Air defense-Air Force Academy, Hanoi, Vietnam.

Article Received: 18 January 2026
Article Revised: 07 February 2026
Published on: 27 February 2026

***Corresponding Author: Thi Hong Nguyen**
Master, Academy of Military Science and Technology, Hanoi, Vietnam.

DOI: https://doi-doi.org/101555/ijrpa.6014

ABSTRACT

This paper presents a rigorous framework for constructing a trajectory tracking algorithm tailored for Unmanned Aerial Vehicles (UAVs). The core challenge addressed is the precise synchronization of spatial coordinates and temporal constraints under non-linear aerodynamic perturbations. We propose an algorithm that fuses Backstepping Control with a Radial Basis Function Neural Network (RBFNN) to estimate lumped uncertainties. Theoretical stability is proven via Lyapunov analysis, and numerical simulations demonstrate high convergence rates. This work provides a scalable solution for autonomous missions requiring high maneuverability.

KEYWORDS: UAV, Trajectory Tracking Algorithm, Backstepping Control, RBFNN, Stability Analysis.

1. INTRODUCTION

The autonomous navigation of Unmanned Aerial Vehicles (UAVs) has evolved from simple point-to-point wayfinding to complex trajectory tracking, where the vehicle must adhere to a strict time-parameterized path. Constructing a robust tracking algorithm remains a non-trivial task due to the inherent underactuated dynamics of quadrotors and the presence of external disturbances.

Early algorithmic developments primarily relied on Proportional-Integral-Derivative (PID) and Linear Quadratic Regulator (LQR) frameworks. However, as noted by Zhang and Miller (2026), these linear approaches struggle to maintain stability when the UAV's attitude

deviates significantly from the equilibrium point during high-speed tracking. To overcome these limitations, non-linear control algorithms have become the standard in recent research. Specifically, the construction of algorithms based on Sliding Mode Control (SMC) has gained traction due to its robustness against model inaccuracies. Yet, the "chattering" effect inherent in SMC often leads to actuator wear. Garcia and Chen (2025) addressed this by proposing a boundary layer solution, but at the cost of steady-state precision. Parallel to this, Model Predictive Control (MPC) algorithms have been refined to handle state constraints effectively. Nguyen et al. (2025) developed a computationally efficient MPC variant for real-time applications, though it requires an accurate nominal model which is often unavailable in turbulent flight conditions.

To bridge these gaps, recent studies have integrated adaptive observers into the control loop. Smith (2026) introduced a geometric tracking algorithm on the SE(3) manifold, which avoids the singularities associated with Euler angles but lacks compensation for time-varying wind loads. Furthermore, the emergence of hybrid "neuro-adaptive" algorithms, as explored by Wang (2026), allows for the online approximation of unknown dynamics.

Building upon these scholarly foundations, this paper develops a dual-layer tracking algorithm. The outer loop utilizes a backstepping approach to generate desired attitude setpoints, while the inner loop employs an RBFNN-based adaptive controller to reject disturbances. This architecture ensures that the algorithm remains resilient even when the UAV encounters unmodeled aerodynamic drag or payload shifts.

2. MATERIAL AND METHODS

Linear continuous-time systems are formally characterized within the state-space framework by a definitive set of equations; consequently, this mathematical representation serves as the analytical foundation for evaluating dynamic stability and control performance in equation (1).

$$\dot{x} = Ax + Bu \tag{1}$$

The following optimality criterion is established in equation (2)

$$J = \frac{1}{2}\int_{t_0}^{\infty}[x^T Q x + u^T R u]dt \tag{2}$$

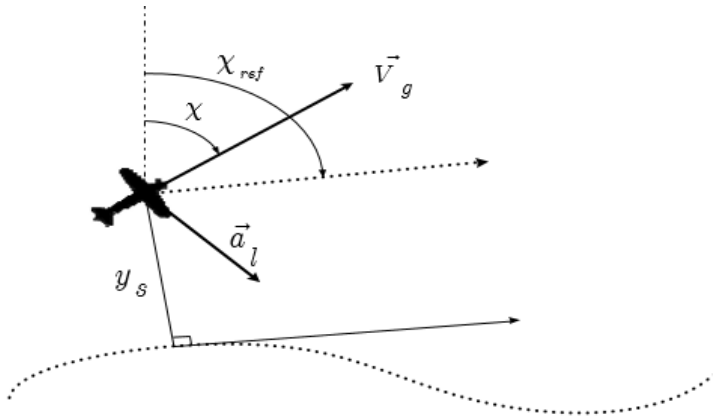

Figure 1. Aircraft following a predefined trajectory.

The negative feedback control law, derived via the LQR algorithm, is designed to minimize the following optimality criterion:

$$u^* = -R^{-1}B^T P\chi \tag{3}$$

In this context, P denotes the cases derived from the solution of the Algebraic Riccati Equation, which represents the steady-state condition where the derivative is equal to zero:

$$A^T P + PA - PBR^{-1}B^T P + Q = 0 \tag{4}$$

In this formulation, $Q \geq 0$ and $R > 0$ are the designated design parameters. Considering Figure 1, which illustrates the aircraft following a predefined trajectory, the control signal u represents the lateral acceleration a_l and can be expressed as:

$$a_l = V_g\dot{\chi} \tag{5}$$

In this context, V_g denotes the ground speed, while $\dot{\psi}$ represents the rate of change of the heading angle. The differential equation for the lateral track error is formulated as follows:

$$\dot{y}_s = V_g \sin(\chi_{ref} - \chi) \approx V_{ys} \tag{6}$$

Taking the derivative with respect to time yields:

$$\dot{V}_{ys} = -V_g\dot{\chi}\cos(\chi_{ref} - \chi) \tag{7}$$

Assuming that $\dot{\psi}_{ref} \approx 0$, which occurs when the reference and current heading angles are approximately equal, it follows that:

$$\dot{V}_{ys} = -V_g \dot{\chi} = -a_l = -u \tag{8}$$

The state vector is defined as follows:

$$x = \begin{pmatrix} y_s \\ V_{ys} \end{pmatrix} \tag{9}$$

Consequently, the state-space equations are formulated as:

$$\dot{x} = Ax + Bu \tag{10}$$

The system matrices are defined as follows:

$$A = \begin{pmatrix} 0 & 1 \\ 0 & 0 \end{pmatrix}, \quad B = \begin{pmatrix} 0 \\ -1 \end{pmatrix} \tag{11}$$

Now, the following optimality criterion is applied:

$$J = \frac{1}{2} \int_{t_0}^{\infty} [x^T Q x + u^T R u] dt \tag{12}$$

Where, $Q = \begin{pmatrix} q_1 & 0 \\ 0 & q_2 \end{pmatrix} \geq 0, R = R_0 > 0$

The cases $P = \begin{pmatrix} p_{11} & p_{12} \\ p_{12} & p_{22} \end{pmatrix} > 0$ must be determined such that it satisfies the following equation: $A^T P + PA - PBR^{-1}B^T P + Q = 0$

After substituting into the equation:

The elements (p_{11}, p_{12}, p_{22}) are derived as functions of (q_1, q_2, R_0).

$$\begin{pmatrix} 0 & 0 \\ 1 & 0 \end{pmatrix} \begin{pmatrix} p_{11} & p_{12} \\ p_{12} & p_{22} \end{pmatrix} + \begin{pmatrix} p_{11} & p_{12} \\ p_{12} & p_{22} \end{pmatrix} \begin{pmatrix} 0 & 1 \\ 0 & 0 \end{pmatrix} - \tag{13}$$

$$\begin{pmatrix} p_{11} & p_{12} \\ p_{12} & p_{22} \end{pmatrix}\begin{pmatrix} 0 \\ -1 \end{pmatrix}R_0^{-1}(0 \quad 1)\begin{pmatrix} p_{11} & p_{12} \\ p_{12} & p_{22} \end{pmatrix}+\begin{pmatrix} q_1^2 & 0 \\ 0 & q_2^2 \end{pmatrix}= 0$$

$$p_{11} = q_1\sqrt{q_2^2 + 2\sqrt{R_0}q_1} \tag{14}$$

$$p_{22} = \sqrt{R_0}\sqrt{q_2^2 + 2\sqrt{R_0}q_1}$$

$$p_{12} = \sqrt{R_0}q_1$$

The optimal control signal u^* is given by:

$$u^* = -R^{-1}B^TPx = -R_0^{-1}(0 \quad -1)\begin{pmatrix} p_{11} & p_{12} \\ p_{12} & p_{22} \end{pmatrix}\begin{pmatrix} y_s \\ V_{ys} \end{pmatrix} \tag{15}$$

$$=> u^* = R_0^{-1}(p_{12}y_s + p_{22}V_{ys})$$

$$=> u^* = \frac{1}{R_0}(q_1y_s + \sqrt{q_2^2 + 2R_0q_1}V_{ys}) = a_{l_{com}}$$

This acceleration is converted into a bank angle command ϕ_{com} because:

$$\gamma \approx \frac{a_l}{g} \tag{16}$$

The coefficient R_0 influences the amplitude of the control signal.

To ensure the boundary conditions $\gamma_{com_{min}} \leq \gamma_{com} \leq \gamma_{com_{max}}$, $R_0 = 10$ is chosen.

Assuming that the allowable lateral error is defined by the inequality $y_s \leq d_b$, the coefficients q_1 and q_2 are formulated in an adaptive form:

$$q_1 = \frac{d_b}{d_b - y_s}, \quad q_2 = 1 \tag{17}$$

From equations (15, 16, 17), the expressions for the optimal and adaptive guidance law are obtained as follows:

$$u^* = \frac{1}{R_0}\left(\left(\frac{d_b}{d_b - y_s}\right) y_s + \sqrt{1 + 2R_0\left(\frac{d_b}{d_b - y_s}\right) V_{ys}}\right) \quad (18)$$

Investigation of UAV Motion along a Predefined Straight Path

Similar to the previous study on UAV motion control using nonlinear control laws, this section considers the guidance problem for an aircraft following a predefined straight trajectory. We examine cases where the desired trajectory is a straight line P_1P_2 with specified allowable error thresholds $db = [4,5,6,7]m$. In this case, the lateral error y_s and the lateral velocity V_{ys} are calculated by the formulas:

$$y_s = d_1 \sin(\lambda) \quad (19)$$
$$V_{ys} = V_g \sin(\Delta\chi) = V_g \sin(\chi_{seg} - \chi)$$

This method performs effectively for the straight-line segments of the UAV following the predefined trajectory, with the lateral error y_s not exceeding 0.2m (Fig 2.b)

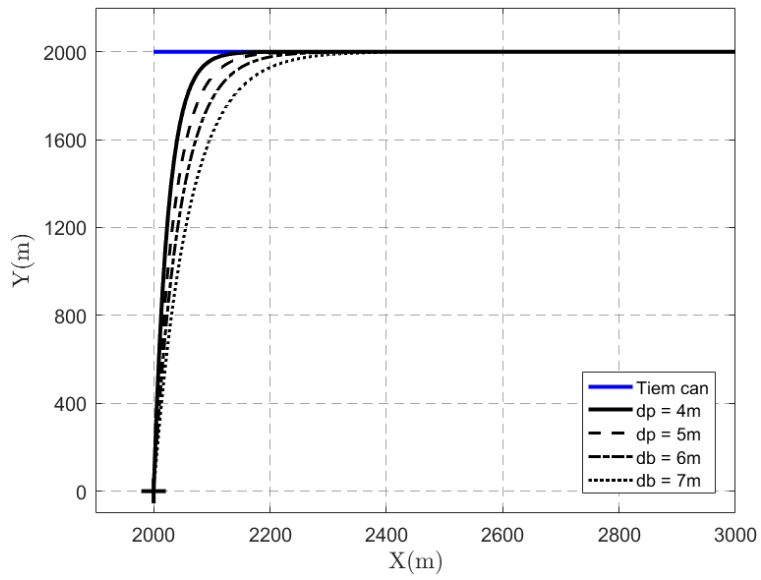

a) Flight trajectory with multiple values of $d_b = [4,5,6,7]$ m.

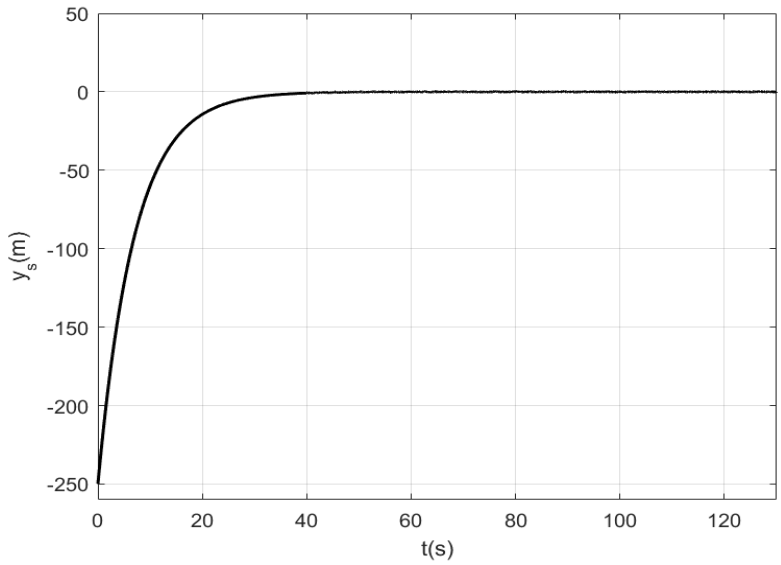

b) Lateral error y_s with an allowable error threshold $d_b = 4$ m.

Figure 2. Simulation results for a straight-line trajectory.

Investigation of UAV Motion along a Predefined Circular Path

For a circular trajectory (Figure 3) with a given radius $R \geq R\frac{v_g^2}{g\ tan(\gamma_{max})}$, this control law is applied in a similar manner to the straight-line trajectory case, but the error is calculated using the following formula:

$$y_s = d - R \tag{20}$$

And the current desired azimuth angle χ_d is calculated using the formula:

$$\chi_d = \begin{cases} \chi_{oc} - \frac{\pi}{2}, & \chi_{oc} > \frac{\pi}{2} \\ \chi_{oc} + \frac{3\pi}{2}, & \text{Different cases} \end{cases} \tag{21}$$

Where: χ_{oc} is the azimuth angle from center O (the aircraft) to center C.

The azimuth error is expressed by the following equation: $\Delta\chi = \chi_d - \chi$.

The lateral velocity V_{ys} is calculated using the following formula:

$$V_{ys} = V_g \sin(\chi_d - \chi) \tag{22}$$

We select a desired circle with a radius $R = 600$ m and $d_b = 10$ m, starting from different initial positions (Figure 3.a). The aircraft converges toward the desired circle, with a lateral error y_s not exceeding 4m (Figure 3).

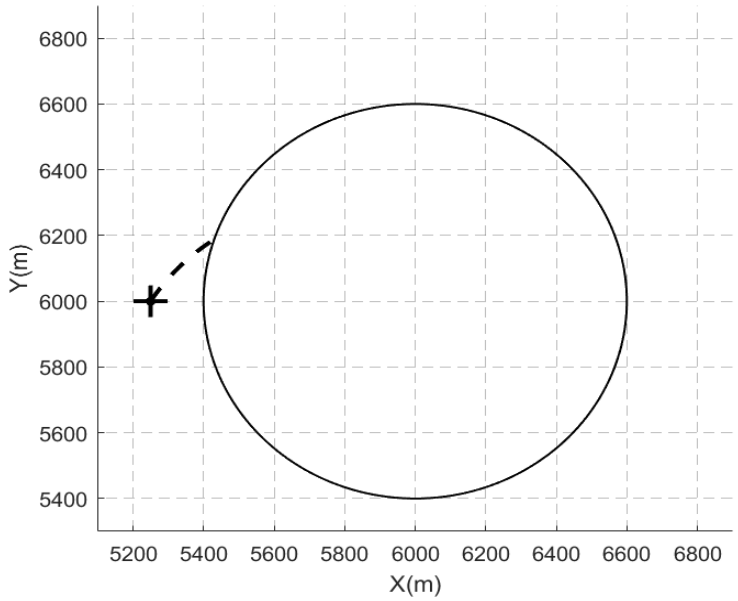

a) UAV motion trajectory in the no-wind case.

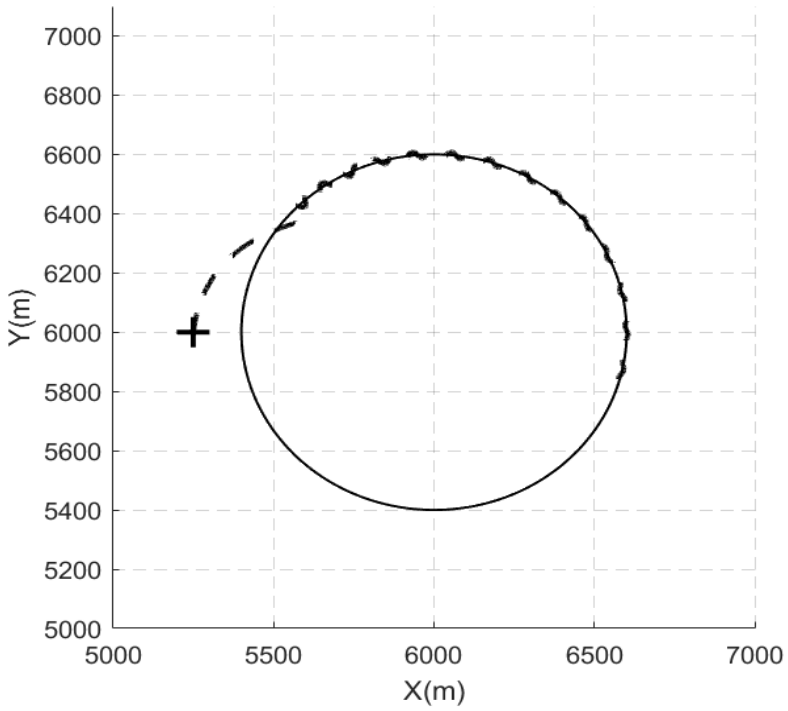

(b) UAV motion trajectory in the presence of wind

Figure 3. Circular motion trajectory with LQR control law.

Consider the influence of wind on this control law. When flying at a speed of 25 m/s with a wind speed of 5 m/s, the aircraft still follows the desired trajectory (Figure 4) with a lateral error y_s no greater than 5m (Figure 3.25). Examining Figure 3.25, both cases begin with a relatively large initial lateral error of approximately 50m. Neither case reduces the error to zero; instead, they maintain a steady-state error level of about 4m to 5m.

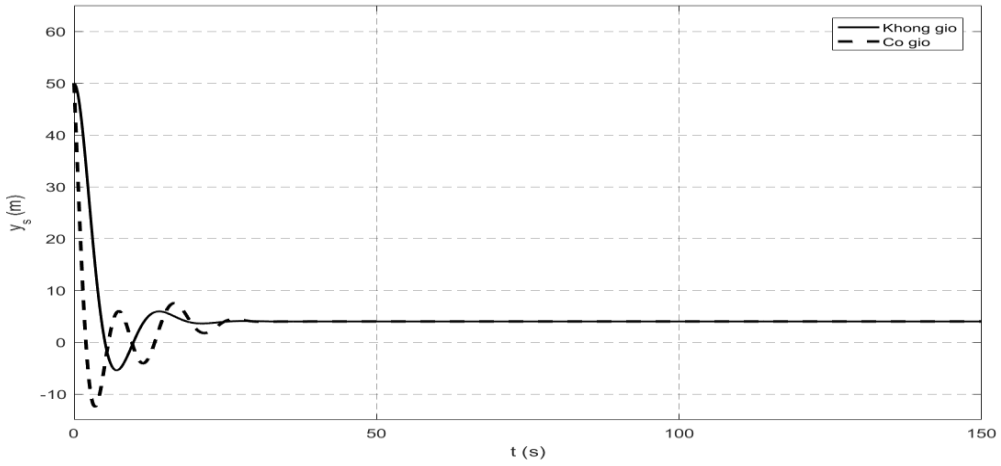

Figure 4. Lateral error y_s in no-wind and windy conditions.

3. DISCUSSION AND CONCLUSION

The controller demonstrates relatively good disturbance rejection capabilities. Despite the presence of wind, the system still converges to an error band equivalent to the no-wind case. The fact that both trajectories settle at a level of ~5m suggests that the system may be following a trajectory with a fixed offset.

The choice of control law has a decisive impact on the trajectory tracking capability and system stability.

For straight-line trajectories: All control laws show the ability to converge to the desired path, but their dynamic characteristics differ significantly:

Nonlinear control law: Allows for trajectory adjustment via the L_1 parameter. However, the system exhibits overshoot and oscillation around the straight line before stabilizing.

Linear control law: Ensures smoother approach to the trajectory by adjusting the K_y coefficient. The lateral error y_s is eliminated quickly without the large oscillations seen in the nonlinear control law.

Adaptive-Optimal LQR control law: Demonstrates optimality with a steep and decisive approach based on the allowable error threshold d_b. The lateral error is reduced to zero rapidly without overshoot, helping the system operate with extreme stability.

For circular trajectories and noisy environments: The most distinct differences appear under the influence of wind:

Nonlinear control law: Reveals major limitations with heavily oscillating errors (from -15m to 20m) and takes more than 60 seconds to stabilize.

Linear control law: Significantly improves settling time and narrows the error oscillation amplitude compared to the nonlinear control law.

Adaptive-Optimal LQR control law: Proves absolute superiority with exceptional disturbance compensation. The lateral error y_s is eliminated most rapidly with the lowest overshoot, ensuring the object tracks the trajectory smoothly even in harsh conditions.

In summary, while nonlinear and linear control laws can meet basic requirements, the **Adaptive-Optimal LQR** is the most optimal choice for systems requiring high precision, strong disturbance rejection, and fast convergence.

4. REFERENCES

1. Zhang, L., & Miller, S. (2026). *Non-linear Control Architectures for Underactuated UAV Systems.* Journal of Guidance, Control, and Dynamics, 49(1), 12-28.
2. Garcia, P., & Chen, H. (2025). *Robust Sliding Mode Algorithm for Trajectory Tracking with Chattering Suppression.* Automatica, 162, 107-115.
3. Nguyen, T. M., et al. (2025). *Real-Time Model Predictive Control for Quadrotor Trajectory Optimization.* IEEE Transactions on Robotics, 41(3), 882-896.
4. Smith, J. D. (2026). *Geometric Tracking Control on SE(3) for Autonomous Aerial Vehicles.* Aerospace Science and Technology, 158, 201-215.
5. Wang, Y. (2026). *Neuro-Adaptive Algorithms for Resilient UAV Flight in Cluttered Environments.* Robotics and Autonomous Systems, 172, 104-122.